Mechanistic Model for Eccentric Annular Gas-Liquid Flow in Horizontal Pipelines

Adriana Brito, Nelson MacQuhae, Francisco García, Nelson Fernández and José Colmenares

Abstract A mechanistic model for the prediction of pressure drop in horizontal pipelines is presented for annular flow. A new empirical correlation for the liquid/wall interfacial friction is proposed, where the effects of the annular flow eccentricity, due to the difference between the fluid density and viscosity, are accounted for. The model is compared to three different correlation models and five mechanistic models in current use. Its accuracy has been validated against experimental data for annular gas-liquid flow in horizontal pipelines, taken from different sources. A number of 240 experiments were carried out with superficial liquid velocities between 0.003 and 5.96 m/s, superficial gas velocities between 9 and 69.6 m/s, liquid viscosities between 1 and 1200 cP, and pipeline diameters between 0.0261 and 0.0953 m. We find that the mechanistic model proposed here reduces the absolute error of the pressure drop prediction by approximately 20 % compared to other mechanistic models.

1 Introduction

The drop of pressure in gas-liquid segregated flow patterns is perhaps the most difficult parameter to predict, while annular flow is one of the most common two-phase flow patterns that arise in practice. The most widely used mechanistic models

A. Brito (✉) · J. Colmenares
Instituto Tecnológico Venezolano del Petróleo (PDVSA-Intevep), Urbanización El Tambor, Los Teques 1201, Estado, Miranda, Venezuela
e-mail: britoah@pdvsa.com

J. Colmenares
e-mail: jcolmenares@cantv.net

N. MacQuhae · F. García · N. Fernández
Escuela de Ingeniería Mecánica, Instituto de Mecánica de Fluidos, Universidad Central de Venezuela, Caracas 1051, Venezuela
e-mail: nelsonm@microsoft.com

N. Fernández
e-mail: nelson.fernandez@ucv.ve

L. Di G. Sigalotti et al. (eds.), *Computational and Experimental Fluid Mechanics with Applications to Physics, Engineering and the Environment*, Environmental Science and Engineering, DOI:10.1007/978-3-319-00191-3_29,

for predicting pressure drops in pipelines are those reported by Xiao et al. (1990), Ouyang et al. (1998), Gómez et al. (1999), and Holden (2002). However, the accuracy of these predictive models against the experimental data is over 45 %.

In annular flow patterns, the relevant parameters for the prediction of the pressure drop are the film distribution, the droplet entrainment in which small drops of one phase remain trapped in the other phase, and the fluid-wall friction factor. Therefore, the aim of this study is to develop a mechanistic model that takes into account all these parameters and reduces the uncertainty in the pressure gradient prediction.

The improved accuracy of the model has been validated against gas-liquid annular flow data from Beggs (1972), Mukherjee (1979), and Andritsos (1986), as well as from experimental data provided by different companies related to the database of the Stanford University and from Petróleos de Venezuela S. A. (PDVSA) for the case of air and heavy oil.

2 Annular Flow Models in Pipelines

In horizontal pipelines, where the film distribution is around the pipe wall and the gas is characterized by its continuity along the core of the pipe, the annular flow tends to be eccentric. The level of eccentricity depends on the density and viscosity of the fluid, as well as on the flow rates of liquid and gas. The liquid film is thinner in the upper than in the lower part of the pipe and the liquid phase moves in a wavy manner close to the gas-liquid interface so that droplets are entrained in the gas core.

In models of gas-liquid eccentric annular flow, a Newtonian two-fluid approach is usually employed, where the liquid film is the liquid phase and the gas-droplet mixture is considered to be the gas phase. We assume that the flow is stationary, incompressible, isothermal, and one-directional. Moreover, we consider the simple case in which there is no mass transfer between the phases and assume that the pressure gradients in the gas and liquid film are the same.

If we start from the continuity equation:

$$\frac{\partial \rho_f}{\partial t} + \nabla \cdot \left(\rho_f \vec{v}\right) = 0, \tag{1}$$

where ρ_f is the mass density and v is the fluid velocity vector, the continuity equation for steady-state flow written in a generalized orthogonal coordinate system reduces to

$$\frac{1}{h_1 h_2 h_3}\left[\frac{\partial}{\partial z}\left(h_1 h_2 v_z\right)\right] = 0, \tag{2}$$

where h_1, h_2, and h_3 are the components of the metric tensor of the orthogonal coordinate system defined as

$$h_1^2 = \left(\frac{\partial x}{\partial \rho}\right)^2 + \left(\frac{\partial y}{\partial \rho}\right)^2 + \left(\frac{\partial z}{\partial \rho}\right)^2,$$
$$h_2^2 = \left(\frac{\partial x}{\partial \phi}\right)^2 + \left(\frac{\partial y}{\partial \phi}\right)^2 + \left(\frac{\partial z}{\partial \phi}\right)^2, \quad (3)$$
$$h_3^2 = \left(\frac{\partial x}{\partial z}\right)^2 + \left(\frac{\partial y}{\partial z}\right)^2 + \left(\frac{\partial z}{\partial z}\right)^2,$$

where (x, y, z) are the three Cartesian-coordinate axes, and $\rho = \rho(x, y), \phi = \phi(x, y)$ are some orthogonal coordinates to be specified later below. In Eq. (2), v_z is the velocity component in the axial (z-axis) direction. In addition, for one-directional flow along the z-axis, the momentum equation becomes

$$0 = -\left(\frac{\partial P}{\partial z}\right) + \rho_f g + \frac{1}{h_1 h_2 h_3}\left[\frac{\partial}{\partial \rho}\left(h_2 h_3 \tau_{\rho z}\right)\right], \quad (4)$$

where P is the pressure, g is the acceleration of gravity, and $\tau_{\rho z}$ is the shear stress in the axial direction. We write the momentum equation in dimensionless form by introducing the following dimensionless parameters:

$$\tilde{\rho} = \frac{2}{D}\bar{\rho} \quad ; \quad \tilde{P} = \frac{D}{2v_o\mu}P \quad ; \quad \tilde{V} = \frac{v_i}{v_o} \quad ; \quad \tilde{\tau}_{\rho z} = \frac{D}{2v_o\mu}\tau_{\rho z} \quad ; \quad \tilde{z} = \frac{2}{D}z \quad (5)$$

where$\bar{\rho}$ is the inner radius derived from the hydraulic diameter of the gas phase, v_i is the velocity at the gas-liquid interface, v_o is the characteristic velocity of the system, μ is the viscosity, and D is the pipe diameter. In the momentum equation for the liquid phase, the parameters v_o and μ are the superficial velocity and the viscosity of the liquid, while in the momentum equation for the gas phase they correspond to the superficial velocity and viscosity of the gas.

For the liquid phase, we use an orthogonal coordinate system, i.e., $(\tilde{\rho}(x, y), \phi(x, y))$, based on the coordinate system proposed by González (1998). This coordinate system arises from a bilinear transformation in non-dimensional form, where the fluid domain is the space confined between the inner diameter (formed by the gas phase), which is less than one, and the outer diameter, which is equal to one.

The eccentric annular flow is mainly affected by the floatation effect of the gas phase and the viscosity of the liquid. In order to represent mathematically this effect it is necessary to use the modified bilinear transformation (see Fig. 1):

$$w = \frac{z^* - ai}{az^* - i}, \quad (6)$$

where a is the transformation pole. Following the procedure given by González (1998), we rotate the bilinear coordinate system and transform to rectangular Cartesian coordinates (x,y) such that $(x(\tilde{\rho}, \phi), y(\tilde{\rho}, \phi))$, where

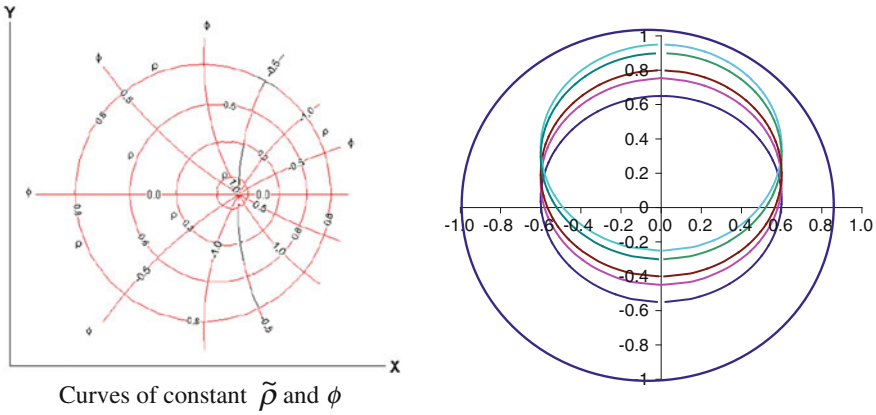

Fig. 1 Orthogonal coordinate system

$$x = \frac{\tilde{\rho}\sin\phi\left(1-a^2\right)}{a^2\tilde{\rho}^2-2a\tilde{\rho}\cos\phi+1},$$
$$y = \frac{a\left(\tilde{\rho}^2+1\right)-\tilde{\rho}\cos\phi\left(1+a^2\right)}{a^2\tilde{\rho}^2-2a\tilde{\rho}\cos\phi+1}. \tag{7}$$

Here$\tilde{\rho}$ is the dimensionless hydraulic inner radius of the gas phase and ϕ is the angle formed by the radial lines from the centre of the circumference ($0 < \varphi < 2\pi$; see Fig. 1).

For the proposed coordinate system the scale factors $h_1, h_2,$ and h_3 for the liquid phase are given by

$$h_1 = \frac{\left(1-a^2\right)}{\left(a^2\tilde{\rho}^2-2a\tilde{\rho}\cos\phi+1\right)}; \quad h_2 = \frac{\tilde{\rho}\left(1-a^2\right)}{\left(a^2\tilde{\rho}^2-2a\tilde{\rho}\cos\phi+1\right)}; \quad h_3 = 1. \tag{8}$$

Substituting the scale factors (8) into the dimensionless form of Eq. (4), we obtain for the momentum equation of the liquid phase

$$0 = -\left(\frac{\partial\tilde{P}}{\partial\tilde{z}}\right)_L - \frac{Re_{SL}}{4\mathrm{Fr}_{SL}}\sin\alpha + \frac{\left(a^2\tilde{\rho}^2-2a\tilde{\rho}\cos(\phi)+1\right)^2}{\left(1-a^2\right)^2\tilde{\rho}} \left[\frac{\partial}{\partial\tilde{\rho}}\left(\frac{\left(1-a^2\right)\tilde{\rho}}{\left(a^2\tilde{\rho}^2-2a\tilde{\rho}\cos(\phi)+1\right)}\tilde{\tau}_{\rho z}\right)\right], \tag{9}$$

where Re_{SL} is the Reynolds number of the liquid phase, Fr_{SL} is the liquid Froude number, and $\tilde{\tau}_{\rho z}$ is the dimensionless shear stress in the axial direction, ie.,

$$Re_{SL} = \frac{\rho_L v_{SL} D}{\mu_L}; \quad \mathrm{Fr}_{SL} = \frac{v_{SL}^2}{gD}; \quad \tilde{\tau}_{\rho z} = \frac{D}{2v_{SL}\mu_L}\tau_{\rho z}. \tag{10}$$

Here v_{SL} is the velocity of the liquid phase, while ρ_L and μ_L are the density and viscosity of the liquid. In order to determine the pressure gradient in the pipe, we integrate Eq. (9) to obtain:

$$\frac{\left(R_i^2-1\right)\left(1-a^4R_i^2\right)}{\left(aR_i-1\right)^2\left(aR_i+1\right)^2}\left(\frac{\partial\tilde{P}}{\partial\tilde{z}}+\frac{Re_{SL}}{4\mathrm{Fr}_{SL}}\sin\alpha\right)_L=\left[2\tau_{zw}-\frac{2R_i\left(1-R_i^2\right)}{\left(1-a^2R_i^2\right)}\tilde{\tau}_{iL}\right], \tag{11}$$

where R_i, $\tilde{\tau}_{zw}$, and $\tilde{\tau}_{iL}$, are, respectively, the dimensionless hydraulic radius of the gas phase in the annular core, the shear stress at the pipe wall for the liquid, and the interfacial shear stress given by

$$R_i=\frac{(e-R_1)-a}{a\,(e-R_1)-1};\quad \tilde{\tau}_{zw}=\frac{D}{2v_{SL}\mu_L}\tau_{zw};\quad \tilde{\tau}_{iL}=\frac{D}{2v_{SL}\mu_L}\tau_i. \tag{12}$$

For the gas phase, we write the momentum equation in cylindrical coordinates and assume that the gas phase is flowing in a perfect cylinder, where its diameter is given by the hydraulic diameter of the gas core in the annular flow pattern. After substitution of the scale factors $h_1=1$, $h_2=\rho$, and $h_3=1$ into Eq. (4), it is possible to obtain the momentum equation for the gas phase in dimensionless form

$$\left(\frac{\partial\tilde{P}}{\partial\tilde{z}}+\frac{Re_{SG}}{4\mathrm{Fr}_{SG}}\sin\alpha\right)_G=-\frac{2}{R_i}\tilde{\tau}_{iG}, \tag{13}$$

where Re_{SG}, Fr_{SG}, and $\tilde{\tau}_{iG}$ are, respectively, the Reynolds and Froude numbers of the gas phase and the dimensionless interfacial shear stress, defined as

$$Re_{SG}=\frac{\rho_C v_{SG}D}{\mu_G};\quad \mathrm{Fr}_{SG}=\frac{v_{SG}^2}{gD};\quad \tilde{\tau}_{iG}=\frac{D}{2v_{SG}\mu_G}\tau_i, \tag{14}$$

where now v_{SG} is the velocity of the gas phase and ρ_G and μ_G refer to the density and viscosity of the gas. The gas core density in the annular flow, ρ_c, is a no-slip density because the core is considered a homogeneous mixture of gas and entrained liquid droplets flowing at the same velocity (Ansari et al. 1994), that is

$$\rho_c=\rho_L H_{Lc}+\rho_G(1-H_{Lc}). \tag{15}$$

The no-slip holdup in the gas core, H_{Lc}, is given by

$$H_{Lc}=\frac{v_{SL}\mathrm{Fe}}{v_{SG}+v_{SL}\mathrm{Fe}}, \tag{16}$$

where Fe is the fraction of the total liquid entrained in the gas core and given by (Oliemans et al. 1986)

$$\frac{\mathrm{Fe}}{1-\mathrm{Fe}} = 10^{\beta_0}\rho_L^{\beta_1}\rho_G^{\beta_2}\mu_L^{\beta_3}\mu_G^{\beta_4}\sigma^{\beta_5}D^{\beta_6}V_{LS}^{\beta_7}V_{GS}^{\beta_8}g^{\beta_9}. \tag{17}$$

In this relation, the exponents β are numbers corresponding to fitted parameters.

On eliminating the pressure gradient from Eqs. (11) and (13), it is possible to obtain the combined momentum equation

$$\tau_i \frac{S_L}{A}\left(\frac{1}{R_i} + \frac{R_i\left(1-a^2\right)}{\left(1-a^2R_i^2\right)}\lambda\right) - \tau_{wL}\frac{S_L}{A}\lambda + g\sin\alpha\left(\rho_G - \rho_L\right) = 0, \tag{18}$$

where A is the cross-sectional area of the pipe, S_L is its perimeter, and λ is a geometric factor that takes into account the effects of the annular flow eccentricity

$$\lambda = \frac{\left(aR_i - 1\right)^2\left(aR_i + 1\right)^2}{\left(1-R_i^2\right)\left(1-a^4R_i^2\right)}. \tag{19}$$

Moreover, the shear stress at the pipe wall for the liquid, τ_{wL}, is defined by

$$\tau_{wL} = \frac{1}{2}f_{wL}\rho_L v_L^2, \tag{20}$$

where f_{wL} is the wall-liquid friction factor, which obeys the experimentally obtained correlation for annular flow

$$f_{wL} = 0.0063 + 53.4662\mathrm{Re}_M^{-1}. \tag{21}$$

In the above relation, Re_M is the Reynolds number proposed by García et al. (2003):

$$Re_M = \frac{\rho_L v_M D}{\mu_L}. \tag{22}$$

Furthermore, the interfacial shear stress, τ_i, is given by

$$\tau_i = \frac{1}{2}f_i\rho_c\left(v_G - v_L\right)^2, \tag{23}$$

where the gas-liquid interfacial friction factor, f_i, is given by Whalley and Hewitt (1978) correlation. They determine the interfacial friction factor by considering an interface roughness ($k = C \pm \Delta h_f$), using Colebrook (1939) equation

$$\frac{1}{\sqrt{f_i}} = -4\log\left[\frac{k/D}{3.7} + \frac{1.255}{Re_{SG}\sqrt{f_i}}\right], \tag{24}$$

where Δh_f is the apparent roughness or wave height and the factor C is the density ratio $C \cong 0.3\left(\rho_L/\rho_G\right)^{0.33}$.

Table 1 PDVSA-Intevep experimental data

Source	Points	Fluids	μ_L (cP)	v_{SL} (m/s)	v_{SG} (m/s)	D (m)	ε/D
Exp-A (2001)	5	Air-kerosene	1	0.11-1.6	28.2-45.7	0.0508	0
Exp-B (2000)	14	Air-oil	500	0.01-0.3	10.1-38.2	0.0508	0
Exp-C (2001)	7	Air-oil	1200	0.85-0.9	7.2-24.4	0.0508	0

Table 2 Stanford University data

Source	Points	Fluids	μ_L (cP)	v_{SL} (m/s)	v_{SG} (m/s)	D (m)	ε/D
Govier and Omer (1962)	5	Air-water	1	0.01-0.1	6.3-16.6	0.0261	0
Ansari et al. (1994)	3	Air-oil	80	0.02-0.3	6.1-13.2	0.0266	1.7E-3
Companies[a]	36	Air-oil	15	0.04-0.5	18.7-69.6	0.0502	3.0E-5
	17	Air-HL	1-25	0.02-2.2	8.0-24.1	0.0381	1.2E-3
	12		3-22	0.03-0.6	23.1-59.5	0.0909	1.7E-5
	4		19	0.11-0.6	40.5-63.4	0.0232	6.5E-5
	8		19	0.10-1.0	34.9-57.1	0.0237	6.5E-5
	73	Air-water	1	0.01-0.5	16.9-61.3	0.0455	0

[a] Data sets are identified as: SU24, SU25, SU28, SU29, SU184, SU187, SU199

Table 3 Tulsa University data

Source	Points	μ_L (cP)	v_{SL} (m/s)	v_{SG} (m/s)	D (m)	ε/D
Andritsos (1986)	36	1-70	0.001-0.56	12.15-30.09	0.0252	0
	3	80	0.004-0.02	14.04-24.65	0.0953	0
Beggs (1972)	5	1	0.02-0.56	15.96-24.97	0.0254	0
	3	1	0.02-0.11	14.85-15.12	0.0381	0
Mukherjee (1979)	9	1	0.03-0.56	11.40-24.06	0.0381	0

3 Experimental Data

The experimental data for the gas-liquid annular flow is made of 240 experimental points of a database containing information from the Stanford Multiphase Flow Database (SMFD), the Tulsa University Fluid Flow Project (TUFFP), and PDVSA-Intevep experiments. The range of operation conditions and fluid properties of each database are summarized in Tables 1, 2, and 3.

In each table, the last colum lists the absolute roughness, ε, in terms of the pipe diameter. The statistical parameters employed in this study are listed in Table 4. They are given by: the average percentage error (E_1) and the average error (E_5), which are related to the agreement between predicted and measured data; the average absolute percent error (E_2) and average absolute error (E_6), which are two of the most important statistical parameters because the negative and positive values do not cancel out; the standard percent deviation (E_3) and standard deviation (E_7), which are related to the scatter of the errors with respect to the average error of the experimental data; and the mean root square percent error (E_4) and the root

Table 4 Statistical parameters

Statistical parameter	Definition	Unit
E_1	$\frac{1}{N}\sum_{I=1}^{N}\left(\frac{\Delta P_{cal}-\Delta P_m}{\Delta P_m}\right)*100$	%
E_2	$\frac{1}{N}\sum_{I=1}^{N}\left\|\left(\frac{\Delta P_{cal}-\Delta P_m}{\Delta P_m}\right)\right\|*100$	%
E_3	$\sqrt{\frac{1}{N-1}\sum_{I=1}^{N}\left(\left(\frac{\Delta P_{cal}-\Delta P_m}{\Delta P_m}\right)-E_1\right)^2}*100$	%
E_4	$\sqrt{\frac{1}{N-1}\sum_{I=1}^{N}\left(\left(\frac{\Delta P_{cal}-\Delta P_m}{\Delta P_m}\right)\right)^2}*100$	%
E_5	$\frac{1}{N}\sum_{I=1}^{N}(\Delta P_{cal}-\Delta P_m)$	Pa/m
E_6	$\frac{1}{N}\sum_{I=1}^{N}\|(\Delta P_{cal}-\Delta P_m)\|$	Pa/m
E_7	$\sqrt{\frac{1}{N-1}\sum_{I=1}^{N}((\Delta P_{cal}-\Delta P_m)-E_5)^2}$	Pa/m
E_8	$\sqrt{\frac{1}{N-1}\sum_{I=1}^{N}((\Delta P_{cal}-\Delta P_m))^2}$	Pa/m

mean square error (E_8), which indicate how close the model prediction is to the experimental data.

4 Results and Discussion

In order to develop a model that takes into account the eccentricity of the annular flow in pipelines, we have carried out a series of experiments in PDVSA-Intevep with an air-oil flow of 400 cP in horizontal pipes. We found that for a constant liquid rate, when the gas rate increases, the eccentricity of the annular flow decreases and eventually tends to zero, as shown in Fig. 2, where the eccentricity is plotted as a function of the gas superficial velocity.

We observe that the eccentricity has no relevant effects on the pressure gradient because when we force the model to predict the pressure gradient with an eccentricity equal to zero, the difference obtained is about ± 1 %. Figure 3 compares the predicted values of the pressure gradient for annular flow with the experimental data listed in Tables 1, 2 and 3 for a gas-liquid system. The average absolute error is 30.5% with an estimated standard deviation of 28.9 %. As we may see, the average absolute error of 60 %, corresponding to the experimental database (147 points), has a deviation less than 30 % over a wide range of fluid properties and pipe diameters.

We also compare the performance of the our model with that of other mechanistic models (MM) as proposed by Xiao et al. (1990), Ouyang et al. (1998), Gómez et al.

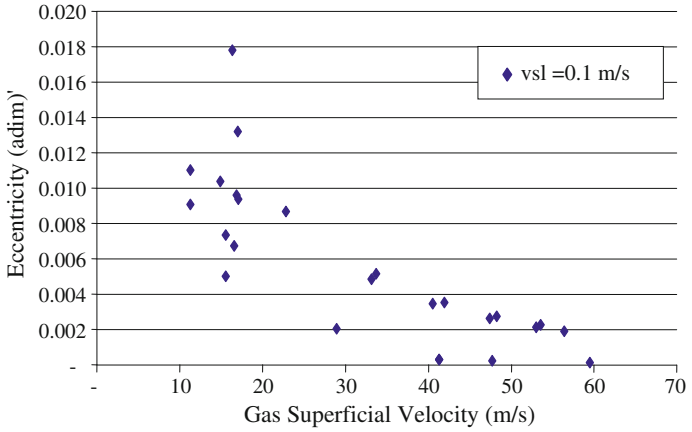

Fig. 2 Eccentricity behaviour of the annular flow

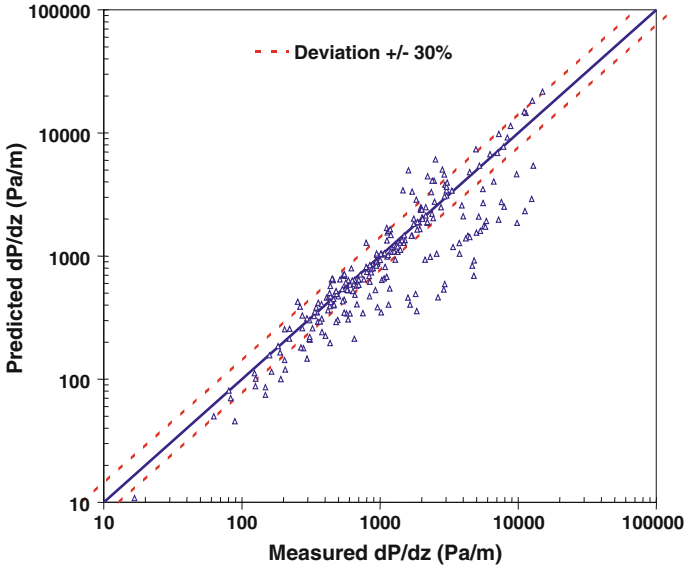

Fig. 3 Comparison of the predicted pressure gradients with existing experimental data

(1999), and Holden (2002) and the correlation models (CM) of Dukler et al. (1964), Beggs and Brill (1973), and García et al. (2003) for the same experimental data of Tables 1, 2 and 3.

The accuracy of the different mechanistic and correlation models is listed in Table 5 and is expressed in terms of the statistical parameters displayed in Table 4. All these models were compared against the experimental data of Tables 1, 2 and 3. We may see that for most existing models in current use the absolute error E_2 is more

Table 5 Comparison of the accuracy of pressure gradient prediction against the experimental data for different mechanistic and correlation models

	E_1 (%)	E_2 (%)	E_3 (%)	E_4 (%)	E_5 (Pa/m)	E_6 (Pa/m)	E_7 (Pa/m)	E_8 (Pa/m)
Garcia CM	−11,8	29,4	31,7	33,8	−127,3	690,6	1444,4	1450,0
Brito MM	−10,3	30,5	40,8	42,1	−354,2	862,0	1780,9	1815,9
Dukler CM	−27,6	31,8	26,6	38,4	−803,3	878,2	1527,8	1726,8
Holden MM	28,4	47,9	118,0	121,4	667,9	1048	5883,6	5921,5
Ouyang MM	−52,8	53,9	25,8	58,7	−1007	1120	1788,9	2053,8
Xiao MM	62,0	92,6	183,7	193,9	33,7	1137	1960,1	1960,4
Beggs and Brill CM	128,9	141,1	554,9	569,8	9578	10108	73313	73939
Gomez MM	164,8	178,9	2023	2030	416,7	1076	4458	4478

than 50 % in the prediction of the pressure gradients for annular flow in pipelines. In contrast, the overall performance of our mechanistic model (Brito MM) yields an absolute error of 30.5 % and so it has a superior accuracy compared to all quoted mechanistic models. We note, however, that the correlation models of Dukler et al. (1964) and García et al. (2003) also produced deviations of about 30 %, similar to our model.

5 Conclusions

A new mechanistic model for the prediction of gas-liquid annular flow in horizontal pipelines has been presented. The accuracy of the model has been assessed by comparing its performance with that of seven different models for a set of 240 experimental points. The main conclusions can be summarized as follows:

- The eccentricity has no important effects on the prediction of the pressure gradients in annular flow patterns, with a difference less than 1 % when concentric and eccentric patterns are considered.
- The limiting case of the model proposed is when the eccentricity is equal to zero (concentric flow).

The present model reduces the absolute error in the prediction of pressure gradients in pipelines by 17 % compared to Holden (2002) mechanistic model, which is considered to be the mechanistic model with better performance. The overall performance of the model is around a 30 % absolute error, similar to the performance obtained with correlation models by Dukler et al. (1964) and García et al. (2003). These results clearly indicate that more studies are indeed required to improve the accuracy of prediction of the physical parameters relevant to annular flow in pipelines.

Acknowledgments This work was performed under the auspices of PDVSA Intevep with the support of the Escuela de Ingeniería Mecánica of the Universidad Central de Venezuela.

References

Andritsos N (1986) Effect of pipe diameter and liquid viscosity on horizontal stratified flow. University of Illinois, Champaign-Urbana, USA, PhD dissertation

Ansari A, Sylvester N, Sarica C, Shoham O, Brill J (1994) A comprehensive mechanistic model for upward two-phase flow in wellbores. SPE Prod Facil 9:142–152

Alves G (1954) Concurrent liquid-gas flow in a pipe-line contactor. Chem Eng Prog 50:449–456

Beggs H (1972) An experimental study of two-phase flow in inclined pipes. University of Tulsa, USA, PhD dissertation

Beggs HD, Brill JP (1973) A study of two-phase flow in inclined pipes. J Petrol Technol 25:607–617

Colebrook CF (1939) Turbulent flows in pipes with particular reference to the transition region between smooth and rough pipe laws. J Inst Civil Eng 11:133–156

Dukler AE, Wicks M, Cleveland RG (1964) Frictional pressure drop in two-phase flow: B. An approach through similarity analysis. AIChE J 10:44–51

García F, García R, Padrino J, Mata C, Trallero J, Joseph D (2003) Power law and composite power law friction factor correlations for laminar and turbulent gas-liquid flow in horizontal pipelines. Int J Multiph Flow 29:1605–1624

Gómez L, Shoham O, Schmidt Z, Chokshi R, Brown A, Northung T (1999) A unified model for steady state two-phase flow in wellbores and pipelines. SPE 56520. In: The 1999 SPE technical conference and exhibition, Houston, Texas, Oct 3–6.

González J (1998) Non-dimensional coordinate system suitable to study flow between two concentric or eccentric cylinders. MSc thesis, The Graduate School, The University of Pittsburgh, USA.

Govier G, Omer M (1962) The horizontal pipeline flow of air-water mixture. Canadian Journal of Chemical Engineering. 40:93

Holden Z (2002) Unified model for gas-liquid pipe flow. Fluid Flow Projects. Ninety ninth research report. Department of Petroleum Engineering, University of Tulsa, USA. Jan 2002.

Mukherjee H (1979) An experimental study of two-phase flow. University of Tulsa, USA, PhD dissertation

Oliemans RV, Pots BFM, Trompé N (1986) Modeling of annular dispersed two-phase flow in vertical pipes. Int J Multiph Flow 12:711–732

Ouyang LB, Arbabi S, Petalas N, Aziz K (1998) Analysis of horizontal well experiments–experiments conducted by Marathon oil for Stanford University's SUPRI-HW program. (SUPRI-B-SUPRI-HW), Stanford University, CA.

Wallis G (1969) One-dimensional two-phase flow. McGraw-Hill, New York

Whalley PB, Hewitt GF (1978) The correlation of liquid entrainment rate in annular two-phase flow. UKAEA report, AERE-R9187, Harwell.

Xiao JJ, Shoham O, Brill JP (1990) A comprehensive mechanistic model for two-phase flow in pipelines. In: The 65th SPE annual technical conference and exhibition, New Orleans, LA. Paper SPE 20631. 167–180, Sept 23–26.